

Quantum Interference in Artificial Band Structures

R. A. Deutschmann, W. Wegscheider,* M. Rother, M. Bichler, and G. Abstreiter
Walter Schottky Institut, Technische Universität München, 85748 Garching, Germany

C. Albrecht and J. H. Smet
Max-Planck-Institut für Festkörperforschung, 70569 Stuttgart, Germany
 (Received 20 June 2000)

Magnetotransport experiments on two-dimensional electron systems with an atomically precise, one-dimensional potential modulation reveal striking quantum interference oscillations. Within a semiclassical framework, they are recognized either as self-interference along closed orbits, many of them rendered possible by magnetic breakdown between Fermi contour segments of the artificial band structure, or as interference-enhanced backscattering. The known commensurability oscillations appear as a special case of the latter mechanism.

DOI: 10.1103/PhysRevLett.86.1857

PACS numbers: 73.61.-r, 71.18.+y, 73.21.-b, 73.50.-h

Abundant new physics was brought about by the invention of the superlattice (SL) concept [1] and its subsequent realization through molecular beam epitaxy (MBE) of layered semiconductor structures with atomic precision. The formation of minibands isolated by minigaps in the vertical SL direction ensues from the coupling between adjacent quantum wells. In order to reduce the dimensionality of the system, electrons are confined in one direction to a quantum well, and a lateral periodic potential modulation may additionally be imposed from the surface of the sample with, for example, lithographically defined top gates. As in the conventional vertical SL geometry, an artificial band structure derives from the reduced width of the Brillouin zone and zone folding. Magnetotransport offers an excellent tool for the study of the resulting band structure in these laterally modulated two-dimensional systems (2DES), since oscillations in the magnetoresistance provide immediate information on the area encircled by closed electron orbits at the Fermi energy E_F [2]. As the magnetic field is raised and if E_F is located within a higher miniband, not only the zero field closed Fermi contours, but also closed trajectories composed of Fermi contour sections belonging to other occupied minibands are traced out by virtue of a tunneling process referred to as magnetic breakdown [3]. All these closed orbits, that encircle different areas, leave signatures in the magnetoresistance and should be instrumental in uncovering the detailed band structure. Contrary to metallic systems, E_F can be tuned over a wide range in these semiconductor based SLs, so that it should in principle be possible to map out the entire energy dispersion.

Surprisingly, to date, such experimental evidence for an artificial band structure is sparse. Only very recently, using two-dimensional modulation, unambiguous proof of two different closed electron orbits was achieved [4]. Similar data for the textbook one-dimensional case has not been reported. This lack of evidence may be related to the inherent inadequacy of lateral modulation schemes in pro-

ducing concurrently a high quality 2DES and a sufficiently short period and large amplitude modulation to guarantee the occupation of only few, well-isolated minibands. Results obtained on semiconductor vicinal surfaces were first thought to exhibit artificial band structure effects, but were later explained in the valley projection model and not as a true superlattice phenomenon [5].

In this Letter, we use a new concept to fabricate lateral SLs based on the cleaved edge overgrowth technique [6], that overcomes the limitations of previous geometries by periodically modulating the material composition *directly adjacent* to the 2DES. In this way, both the period and the modulation strength can be tailored with unprecedented precision by MBE growth. Our magnetotransport data reveal oscillations, that we unambiguously relate to the artificial band structure with a semiclassical theory. These features originate either from self-interference along closed electron orbits, in part made possible through the mechanism of magnetic breakdown, or from quantum interference between open electron paths. Surprisingly, the well-known commensurability oscillations (COs) [7] emerge in our theoretical description as a special class of the latter interference effect. This direct theoretical relationship between Fermi surfaces and these COs had been elusive to this date [8].

The sample structure is shown in Fig. 1. In a first MBE step, an undoped SL with lattice constant $d = 100$ nm of 30 periods of 50 nm GaAs and 50 nm $\text{Al}_{0.32}\text{Ga}_{0.68}\text{As}$ is grown between two n^+ -GaAs contacts, that act as source and drain. In a second MBE step, the sample is cleaved *in situ* and immediately thereafter overgrown by a 30 nm undoped GaAs layer, a 100 nm AlAs barrier, and an n^+ -GaAs gate contact. Similar samples with 15 nm period are discussed in Ref. [9]. By applying a positive gate voltage with respect to source and drain a 2DES is induced at the GaAs/AlAs heterointerface. The finite overlap of the electron wave function with the SL causes a modulation of the electron density n_s in x direction with a strength

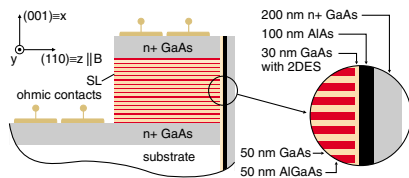


FIG. 1 (color). Sample cross section. The 2DES is field induced at the GaAs/AlAs heterointerface in the (110) direction by means of a positive voltage applied to the $n+$ GaAs gate. The (001)-oriented SL provides an atomically precise potential modulation to the 2DES.

that depends on the GaAs layer thickness. For our sample this variation of the density, integrated over the z direction, exceeds 10%, as determined by a self-consistent 2D-Poisson/Schrödinger calculation. Magnetotransport data, with the magnetic field oriented perpendicular to the 2DES, are obtained at 0.3 K with lock-in techniques.

A typical measurement of the magnetoresistance at a fixed electron density of $3.1 \times 10^{11}/\text{cm}^2$ is depicted in Fig. 2. The trace is plotted against inverse magnetic field, $1/B$, and the resistance values are multiplied by $1/B^2$ to ensure that the small amplitude oscillations at the weakest magnetic fields are made visible. The observed oscillations are all $1/B$ -periodic and four different oscillation frequencies Δ^{-1} can be distinguished in this presentation of the data. Three different frequencies clearly dominate the regimes $1/B > 9.6 \text{ T}^{-1}$, $9.6 \text{ T}^{-1} > 1/B > 6.0 \text{ T}^{-1}$, and $1/B < 6.0 \text{ T}^{-1}$, while in the latter regime an additional beating pattern with a smaller frequency is apparent in the envelope (dashed line). The same experiment is repeated by recording the magnetoresistance from $B = 0$ to 1.4 T and systematically varying the electron density between $n_s = 0.45 \times 10^{11} \text{ cm}^{-2}$ and $n_s = 4.6 \times$

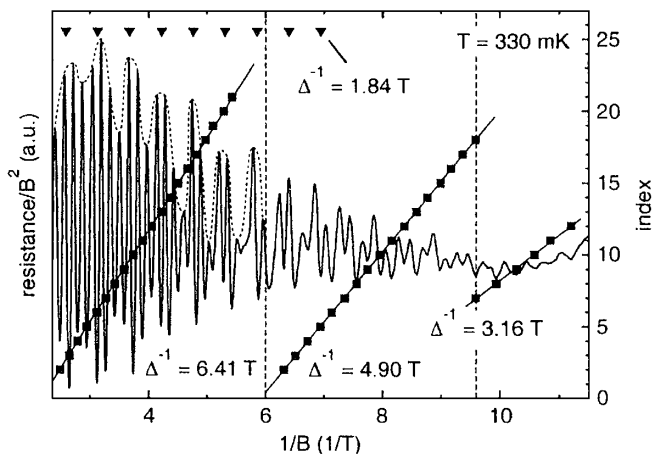


FIG. 2. Typical magnetoresistance curve as a function of the inverse magnetic field. Three different oscillation frequencies are observed in the regimes separated by the dashed lines. Moreover, the envelope exhibits a beating pattern with maxima at the positions of the triangles. For example, at an inverse field of 6.0 T^{-1} the amplitude of the oscillations and the total resistance are 19 and 260Ω , respectively.

10^{11} cm^{-2} . Each curve is then Fourier transformed with respect to the inverse field to obtain the frequency components Δ^{-1} of the magnetoresistance oscillations. The results are summarized in Fig. 3. The amplitudes of the frequency components are plotted on a logarithmic color scale, where large and small amplitudes appear as red and blue, respectively.

To analyze the transport data, the contours of constant energy E_F of the modulated 2DES are plotted with the information acquired from a self-consistent band structure calculation, while keeping in mind the free electron motion along the y direction. Hereafter, minibands are assigned an index n that runs from 0 for the energetically lowest lying miniband to N for the last, partially filled miniband. The minibands with index n and $n + 1$ are separated by the minigap denoted as E_n at $k_x = \pm\pi/d$ or $k_x = 0$. For the density range covered in this experiment three to six minibands are occupied, and the case of four minibands ($n = 0, \dots, 3; N = 3$) is shown in Fig. 4(a). The Fermi contours are color coded and indexed according to the miniband they are associated with. In general, Fermi contour N is closed [red contour in Fig. 4(a)], whereas all other contours ($0, \dots, N - 1$) describe open electron trajectories. The electrons trace these contours in a direction fixed by the sign of the magnetic field. A transition from contour n to its neighbor $n + 1$ entails quantum mechanical tunneling across the gap of size E_n , a process referred to as magnetic breakdown [3]. The tunneling probability $p_n(B)$ depends on E_F and E_n . It vanishes at $B = 0$ and increases exponentially with B . At the lowest B values, the only possible closed electron orbit is along contour N . As B is raised, though, other closed orbits, composed of segments of contour N as well as segments of open contours with lower index, become possible by virtue of magnetic breakdown. In particular the orbit (hereafter

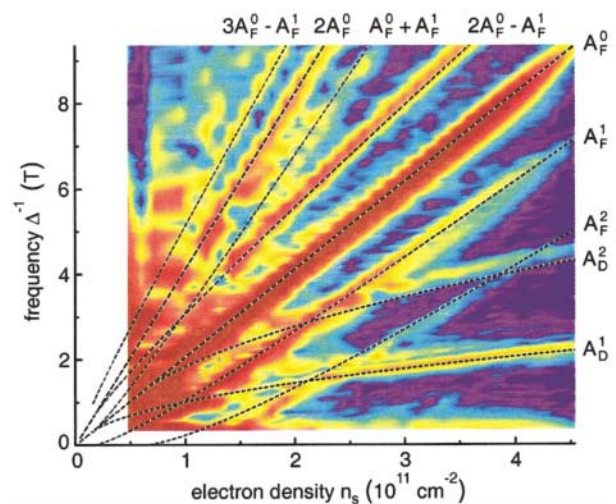


FIG. 3 (color). Color scale plot of the Fourier transformed magnetoresistance data. The density dependent peaks are directly related to different electron trajectories in the artificial band structure.

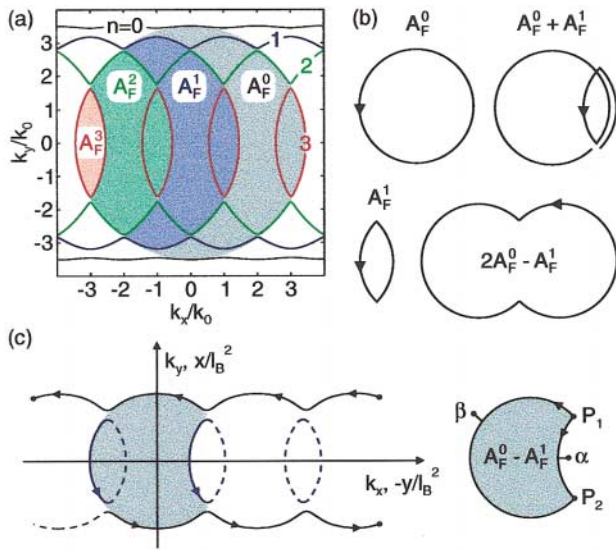


FIG. 4 (color). (a) Fermi contours calculated for $E_F = 7.5$ meV, which is in the fourth miniband. For the sake of clarity, we have chosen larger gaps in this example than obtained from the self-consistent Poisson/Schrödinger calculation for this experiment. Schematic drawing of closed (b) and interfering open (c) orbits responsible for the observed magnetoresistance oscillations.

classified according to the lowest contour index n involved), that descends from the closed Fermi contour associated with miniband n before the Fermi energy was raised from miniband n into miniband N , is reactivated. This closed electron path n shares segments of contours n to N and requires a total of $4 \times (N - n)$ tunnelling events across gaps of size E_n to E_{N-1} . The product of the corresponding $p_i(B)$ factors determines its probability [10]. This orbit encloses an area A_F^n that can be calculated to a very good approximation in the limit $V_0 \rightarrow 0$:

$$A_F^n = 2k_F^2 \left(\arccos\left(n \frac{k_0}{k_F}\right) - n \frac{k_0}{k_F} \sqrt{1 - \left(n \frac{k_0}{k_F}\right)^2} \right), \quad (1)$$

where k_F is the Fermi wave number and $k_0 = \pi/d$. In Fig. 4(a), the closed orbit $n = 1$ contains sections of contours $n = 1, 2$, and 3 , involves tunneling across E_1 and E_2 and encircles the blue shaded area A_F^1 (orbits $n = 2$ in green and 3 in red cover part of this area). According to Onsager [2], electrons that orbit around an arbitrarily shaped Fermi surface A_F give rise to $1/B$ -periodic oscillations in the magnetoresistance with a frequency Δ^{-1} ,

$$\Delta^{-1} = \frac{\hbar}{2\pi e} A_F. \quad (2)$$

Our density dependent study in Fig. 3 of the frequency components contained in the magnetoresistance together with Eqs. (1) and (2) now enables us to identify the maxima marked A_F^0 , A_F^1 , and A_F^2 as caused by electrons performing closed orbits $n = 0, 1$, and 2 . The switch from lower to higher frequency near $B = 104$ mT and $B = 167$ mT in Fig. 2 can be understood as a transition from

electrons orbiting predominantly around the area A_F^2 to orbits around A_F^1 and A_F^0 , respectively. In the intermediate B -field regime multiple closed paths may simultaneously have a significant probability. Eventually all tunneling probabilities approach unity for sufficiently large fields and the orbit with area A_F^0 , equivalent to the cyclotron orbit of the unmodulated 2DES that brings about the commonly known Shubnikov-de Haas oscillations, is restored and prevails. The orbits with area A_F^n are the most obvious closed trajectories, however more complicated closed paths with these simple surfaces as constituents are illustrated in Fig. 4(b) and are in fact resolved in Fig. 3 (for example, $A_F^0 + A_F^1$ and $2A_F^0 - A_F^1$).

Hitherto, the discussed oscillations were a direct consequence of the constructive self-interference of the wave function along *closed* orbits and the subsequent quantization in a magnetic field [2]. This mechanism leaves unexplained our observation of the frequency components determined by the surfaces $A_D^1 = A_F^0 - A_F^1$ and $A_D^2 = A_F^0 - A_F^2$ in Fig. 3, since an electron circling along the closed boundary of this surface would violate the chirality imposed by the B field along part of the perimeter. We assert that oscillations with such frequencies originate from the $1/B$ -periodic modulation of the backscattering probability due to quantum-mechanical interference between two open trajectories with common start and end points as illustrated in Fig. 4(c) for surface A_D^1 . Electrons traveling in negative k_x direction from point P_1 follow either path α or β , depending on whether they do or do not tunnel at this starting point, and rejoin at point P_2 . Constructive interference of the coherent superposition of both paths maximizes the backscattering probability and, consequently, the conductivity σ_{yy} approaches a minimum. It is straightforward to show from the tensor inversion, that this implies a minimum in the longitudinal resistivity ρ_{xx} as well. In the case of destructive interference, the electron will effectively proceed along the open Fermi contour and thus σ_{yy} and ρ_{xx} reach their maximum value. This qualitatively different interference phenomenon reminds one of an Aharonov-Bohm interferometer with the important disparity that in the case at hand the area in real space enclosed by the interfering paths scales with B^{-2} , since real space orbits have the same shape apart from a $\pi/2$ rotation as their counterparts in reciprocal space but are scaled with the square of the magnetic length, $l_B^2 = \hbar/(eB)$. As a result, one anticipates a $1/B$ -periodic rather than a B -periodic phase difference between the interfering trajectories. The phase accumulated along path $i = \alpha$ or β is given by

$$\Phi_i = \frac{1}{\hbar} \int_i (\hbar \vec{k} - e \vec{A}) d\vec{r} + \frac{\pi}{2} C_i, \quad (3)$$

where $-e$ is the electron charge, \vec{A} the vector potential, and C_i a constant. As a result, the B -dependent contribution to

the phase difference $\Phi_D = \Phi_\beta - \Phi_\alpha$ is equal to $l_B^2 A_D^{\beta-\alpha}$, where $A_D^{\beta-\alpha}$ is the area in reciprocal space bounded by a pair of paths α and β . The area $A_D^{\beta-\alpha}$ is nothing but the difference between surfaces A_F^i and A_F^j , that have common borders except for paths α and β . The alternation frequency of the backscattering probability is then obtained from the condition $l_B^2 A_D^{\beta-\alpha} = 2\pi m$ ($m = 1, 2, \dots$), i.e., from Eq. (2) when substituting $A_D^{\beta-\alpha}$ for A_F . Now, it is clear that this quantum interference effect explains the remaining peaks in Fig. 3 marked A_D^1 and A_D^2 .

From Eq. (1), it follows that $4k_F\pi/d$ is a very good approximation of A_D^1 for the density range covered in the experiment of Fig. 3 and is exact in the high density limit. Strikingly, the resulting periodicity is identical to the one of the well-known Weiss oscillations [7], that can be understood in a semiclassical picture: whenever the lattice period d is commensurate with the free electron cyclotron radius R_c in accord with $2R_c = (m - 1/4)d$, ρ_{xx} reaches a minimum. In this expression, the term equal to $1/4$ fixes the absolute position on the magnetic field axis. Noting that Eq. (2) with $A_D^{\beta-\alpha}$ instead of A_F remains valid, the problem of interfering open trajectories can be treated *formally* as self-interference along an imaginary closed orbit. The absolute position of the minima in our interference picture is then obtained when keeping track of *all* contributions to the phase difference $\Phi_D = l_B^2 A_D^1 + \gamma_D\pi/2$, including the Maslov index [11] γ_D associated with the “closed” path. To reach the same result as for Weiss oscillations, γ_D should be equal to 1. For the sake of comparison, we point out that for self-interference along the free cyclotron orbit $\Phi_0 = l_B^2 A_F^0 + \gamma_0\pi/2$, with Maslov index $\gamma_0 = -2$. Since the topology of the imaginary closed orbit is different from the free cyclotron orbit, the difference in their Maslov indices does not come as a surprise. To provide further support for the relationship between COs and the special case of quantum interference between open orbits bounding area A_D^1 , it is instructive to derive the temperature scale up to which this interference phenomenon persists. To this end, the energy variation δE at fixed B inducing a phase change of 2π is calculated,

$$\delta E = \frac{2\pi eB}{\hbar} \left(\frac{\partial A}{\partial E} \right)^{-1} = 2\pi \hbar \omega_c k_F \left(\frac{\partial A}{\partial k_F} \right)^{-1}, \quad (4)$$

where $\hbar\omega_c$ is the free electron cyclotron energy and A the relevant k -space area. For the free electron cyclotron orbit with area $A_F^0 = \pi k_F^2$ the familiar condition $k_B T < \delta E_0 = \hbar\omega_c$ is retrieved from this formula. In contrast, a much weaker temperature dependence is predicted for the interfering open orbits bordering A_D^1 , and the oscillations survive as long as $k_B T < \hbar\omega_c k_F d/2$. This weak temperature dependence is in fact also found in the conventional CO picture [12].

This work on semiconductor SLs bridges the gap with quantum interference phenomena previously reported in metals [13] and more recently in organic superconductors [14]. The fabrication of a device with few occupied minibands enabled the unambiguous demonstration of the artificial band structure through the observation of multiple closed orbits and $1/B$ periodically enhanced backscattering related to quantum interference of open orbits. We have engineered a close to ideal lateral superlattice, which excels in many ways over standard designs due to the unparalleled combination of attractive features: virtually no limitations on modulation period and strength, monolayer precision of the superlattice, exceptional density tunability, and high quality due to the absence of modulation doping. The stage is set for finding further exciting physics at even smaller modulation periods.

We would like to thank P. Vogl, R. R. Gerhardtts, and M. Brack for helpful discussions. This work has been supported by the DFG via SFB 348 and the BMBF under Contracts No. 01BM912 and No. 01BM919/5.

*Present address: Universität Regensburg, Naturwissenschaftliche Fakultät II, 93040 Regensburg, Germany.

- [1] L. Esaki and R. Tsu, IBM J. Res. Dev. **14**, 61 (1970).
- [2] L. Onsager, Philos. Mag. **43**, 1006 (1952).
- [3] M. H. Cohen and L. M. Falicov, Phys. Rev. Lett. **7**, 231 (1961); E. I. Blount, Phys. Rev. **126**, 1636 (1962).
- [4] C. Albrecht *et al.*, Phys. Rev. Lett. **83**, 2234 (1999).
- [5] T. Cole, A. A. Lakhani, and P. J. Stiles, Phys. Rev. Lett. **38**, 722 (1977); T. G. Matheson and R. J. Higgins, Phys. Rev. B **25**, 2633 (1982); L. J. Sham *et al.*, Phys. Rev. Lett. **40**, 472 (1978); T. Ebelbauer *et al.*, Z. Phys. B **64**, 69 (1986).
- [6] H. L. Stormer *et al.*, Appl. Phys. Lett. **58**, 726 (1991); Y. Ohno *et al.*, Phys. Rev. B **52**, R11 619 (1995).
- [7] D. Weiss *et al.*, Europhys. Lett. **8**, 179 (1989); R. R. Gerhardtts, D. Weiss, and K. v. Klitzing, Phys. Rev. Lett. **62**, 1173 (1989); R. W. Winkler *et al.*, *ibid.* **62**, 1177 (1989); C. W. J. Beenakker, *ibid.* **62**, 2020 (1989); C. Zhang and R. R. Gerhardtts, Phys. Rev. B **41**, 12 850 (1990).
- [8] The commensurability oscillations can not only be derived in the low field breakdown regime from the zero field miniband structure as suggested here but also in the high field magnetic breakdown regime as demonstrated in P. Štředa and A. H. MacDonald, Phys. Rev. B **41**, 11 892 (1990).
- [9] R. A. Deutschmann *et al.*, Physica (Amsterdam) **6E**, 561 (2000); R. A. Deutschmann *et al.*, Physica (Amsterdam) **7E**, 294 (2000).
- [10] A. B. Pippard, Proc. R. Soc. London A **270**, 1 (1962); L. M. Falicov and H. Stachowiak, Phys. Rev. **147**, 505 (1966).
- [11] M. Brack and R. K. Bhaduri, *Semiclassical Physics* (Addison-Wesley, Reading, MA, 1997).
- [12] P. H. Beton *et al.*, Phys. Rev. B **42**, 9689 (1990).
- [13] R. W. Stark and C. B. Friedberg, Phys. Rev. Lett. **26**, 556 (1971).
- [14] J.-Y. Fortin and T. Ziman, Phys. Rev. Lett. **80**, 3117 (1998).